Jpn. J. Appl. Phys. Vol. 42 (2003) pp. 4804–4808
Part 1, No. 7B, July 2003

Electrical Pump and Probe Measurements of a Quantum Dot in the Coulomb Blockade Regime

Toshimasa FUJISAWA[1,*], David Guy AUSTING[1,†], Yoshiro HIRAYAMA[1,2] and Seigo TARUCHA[1,3,4]

[1]*NTT Basic Research Laboratories, NTT Corporation, 3-1 Morinosato-Wakamiya, Atsugi 243-0198, Japan*
[2]*CREST Interacting Carrier Electronics Project, 4-1-8 Honmachi, Kawaguchi 331-0012, Japan*
[3]*University of Tokyo, Bunkyo-ku, Tokyo 113-0033, Japan*
[4]*ERATO Mesoscopic Correlation Project, 3-1 Morinosato-Wakamiya, Atsugi 243-0198, Japan*

(Received January 16, 2003; accepted for publication March 18, 2003)

We describe two kinds of electrical pump and probe measurements to investigate energy relaxation time in a quantum dot in the Coulomb blockade regime. Transient current driven by single-step pulses can be used to determine the tunneling rates for the two tunneling barriers as well as the relaxation rate under a limited condition. A double-step pulse scheme is more useful for deducing longer relaxation times. The feasibility of these techniques is demonstrated by simple simulations based on rate equations that describe the time-dependent transport, and by experiments performed on a few-electron quantum dot.
[DOI: 10.1143/JJAP.42.4804]

KEYWORDS: pump and probe measurement, quantum dot, Coulomb blockade, energy relaxation

1. Introduction

A quantum dot (QD) is a small conductive island in which electrons occupy discrete energy states.[1)] Energy relaxation from an excited state (ES) to a ground state (GS) in a QD is an important characteristic for understanding the dynamics of a QD system. Analyses of conventional single electron tunneling current suggest that some unknown excited states show long relaxation time.[2)] Recent time-dependent transport experiments have clearly revealed an extremely long spin-flip relaxation time and relatively short momentum relaxation time in a QD.[3)] When the energy relaxation is inefficient, excess energy, which can be even higher than the excitation energy of the transport, can remain in a QD. Long-lived spin states can cause spin-blockade phenomena and nonequilibium transport, which actually breaks down the single electron tunneling scheme.[4)] Moreover, the energy relaxation time, which is often called longitudinal relaxation time, or T_1, in spin dynamics, is an important parameter to describe how strongly the quantum system is coupled to the environment.[5)] In order to obtain a well-isolated quantum system, which is desired for future quantum information technologies, relaxation time should be investigated in many materials and structures under various conditions. In this paper, we describe two electrical pump and probe measurement schemes in detail, and discuss the feasibility of measuring relaxation time as well as tunneling rates.

2. Electrical Pump and Probe Measurements

We consider a QD in the Coulomb blockade (CB) regime, where the number of electrons in the QD can be fixed at an integer, N. When a gate voltage is immediately changed from one CB region at $N = N_0$ to another at $N = N_0 + 1$, one electron is injected into the QD, and when the gate voltage is changed from $N = N_0 + 1$ to $N = N_0$, one electron is extracted from the QD. These injections and extractions can be performed with a time accuracy approximately given by the inverse of their tunneling rates, Γ^{-1}, which can be varied in a wide range from $\sim$1 ps to $\sim$1 μs for typical QDs. Moreover, an electron can be (sometimes selectively) injected into, or extracted from, the GS or ESs by adjusting external voltages. Therefore, one can design a waveform of the gate voltage to measure the energy relaxation time and the tunneling rates. We can repeatedly apply voltage pulses to push the system out of equilibrium, and measure the time-integrated nonequilibrium transient current in the following two ways.

2.1 Single-step pulse measurement

A very simple scheme is to apply a rectangular-shaped voltage-pulse to a gate electrode, as schematically shown in Figs. 1(a) and 1(b).[6)] For simplicity, we consider energy relaxation from the first ES to the GS for an N_0-electron QD, and neglect higher ESs. For proper measurement, we consider strong asymmetric tunneling barriers, whose tunneling rates are $\Gamma_L \gg \Gamma_R$, under a relatively large source-drain bias voltage $|eV_{sd}| \gg \hbar\Gamma_L$. The polarity of the bias voltage is chosen so that an electron is injected from the

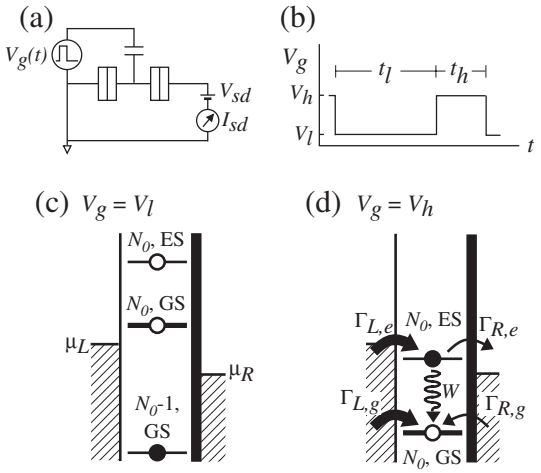

Fig. 1. (a) Diagram of the electrical pump and probe experiment for a quantum dot. (b) Schematic waveform of the single-step pulse. (c) Energy diagram during the low gate voltage. (d) Energy diagram during the high gate voltage. Possible tunneling processes and relaxation path are shown by arrows; thick (thin) arrows for the fast (slow) tunneling processes and a wavy arrow for the relaxation.

*E-mail address: fujisawa@will.brl.ntt.co.jp
†Present address: National Research Council of Canada, Ottawa, Ontario K1A 0R6, Canada.

thinner barrier at a faster rate Γ_L and an electron is extracted from the thicker barrier at a slower rate Γ_R. (We refer to this situation as forward bias.)

First, we prepare a QD in the $N_0 - 1$ electron GS by adjusting the gate voltage at $V_g = V_l$ in the $N_0 - 1$ CB region for a sufficiently long period, $t_l \gg \Gamma_L^{-1}$. In this situation, both the N_0-electron ES and the GS are energetically located above the chemical potential of the electrodes, μ_L and μ_R, as shown in Fig. 1(c). Then, the gate voltage is immediately, but adiabatically, changed to $V_g = V_h$ in the N_0-electron CB region. The rise time of the voltage pulse should be comparable to or shorter than Γ_L^{-1} to see the following effect, but we only consider the adiabatic condition, in which the voltage changes slowly so as not to shake up the quantum system. The high voltage $V_g = V_h$ is adjusted so that only the N_0-electron ES is located between μ_L and μ_R (transport window), as shown in Fig. 1(d). All the possible tunneling processes and the energy relaxation process are shown by arrows. A relatively large source-drain voltage, $|V_{sd}| \gg \hbar\Gamma_L$, is applied in order to eliminate backward tunneling processes, such as tunneling from the N_0-electron ES to the source electrode, which would degrade the relaxation time measurement.

When a pulse is applied, an electron enters either the N_0-electron ES or the GS with probabilities, $\Gamma_{L,e}$ and $\Gamma_{L,g} + \Gamma_{R,g}$, respectively, but only one electron can enter the dot at a time. If an electron enters the ES, it can relax to the GS, or tunnel to the drain electrode to give a net current. However, the transport is blocked once the GS is occupied. Because of the strongly asymmetric barriers, $\Gamma_L \gg \Gamma_R$, an electron can stay in the ES for a relatively long time $\sim\Gamma_R^{-1}$, during which relaxation may take place. The transport through the ES may be terminated by the relaxation process. Therefore, the transport is sensitive to the relaxation time, if the relaxation time is longer than the injection time Γ_L^{-1} but shorter than the extraction time Γ_R^{-1}. This transient transport can be considered as a kind of pump and probe measurement. An electron is pumped into the ES within Γ_L^{-1} after the rising edge of the pulse, and then the electron in the ES is continuously probed by the slow tunneling rate Γ_R^{-1} until it becomes empty.

To clarify this scheme, we analyze this nonequilibrium transport by using simple rate equations. We assume $t_l \gg \Gamma_L^{-1}$, so no excess electron exists in the QD at the beginning of the pulse at $t = 0$. The nonequilibrium transport at the high voltage is described by the rate equations

$$\begin{aligned} \frac{d}{dt}\rho_e &= \Gamma_{L,e}(1 - \rho_e - \rho_g) - \Gamma_{R,e}\rho_e - W\rho_e \\ \frac{d}{dt}\rho_g &= (\Gamma_{L,g} + \Gamma_{R,g})(1 - \rho_e - \rho_g) + W\rho_e, \end{aligned} \tag{1}$$

in which all the tunneling processes shown by arrows in Fig. 1(d) are taken into account. Here, ρ_e and ρ_g are the average electron numbers in the ES and the GS, respectively. $\rho_e = \rho_g = 0$ at $t = 0$, and $0 \le \rho_e + \rho_g \le 1$ is satisfied due to CB. The average number of tunneling electrons, $\langle n_h \rangle$, during a duration, t_h, for the high voltage is given by

$$\langle n_h \rangle = \int_{t=0}^{t_h} [\Gamma_{R,e}\rho_e - \Gamma_{R,g}(1 - \rho_e - \rho_g)]dt. \tag{2}$$

The first term of the integrant describes the probing current from the ES to the drain, while the second term is a stray transport from the drain to the GS and gives a minor effect to the forward bias condition. At the end of the pulse at $t = t_h$, an electron can remain in the ES and GS with the probability $\rho_e(t_h)$ or $\rho_g(t_h)$, respectively. When the gate voltage is changed to low V_l, the residual transport is described by the rate equations

$$\begin{aligned} \frac{d}{dt}\rho_e &= -(\Gamma_{L,e} + \Gamma_{R,e} + W)\rho_e \\ \frac{d}{dt}\rho_g &= -(\Gamma_{L,g} + \Gamma_{R,g})\rho_g + W\rho_e, \end{aligned} \tag{3}$$

with the initial conditions $\rho_e(t_h)$ and $\rho_g(t_h)$. The average number of tunneling electrons, $\langle n_l \rangle$, during a sufficiently long period of low voltage, t_l, which is replaced with infinity, is given by

$$\langle n_l \rangle = \int_{t=t_h}^{\infty} [\Gamma_{R,e}\rho_e + \Gamma_{R,g}\rho_g]dt. \tag{4}$$

Therefore, the total number of tunneling electrons per pulse is obtained by

$$\langle n(t_h) \rangle = \langle n_h \rangle + \langle n_l \rangle. \tag{5}$$

Although the analytical expression of eq. (5) contains different exponential terms, all curves can be approximated by a single exponential curve. Figure 2(a) shows the variation of $\langle n(t_h) \rangle$ for various relaxation rates, $W = 10^3$–10^7 Hz, under the conditions of $\Gamma_{L,e} = \Gamma_{L,g} = 10^9$ Hz and $\Gamma_{R,e} = \Gamma_{R,g} = 10^6$ Hz. The initial slope at $t_h = 0$ is approximately given by

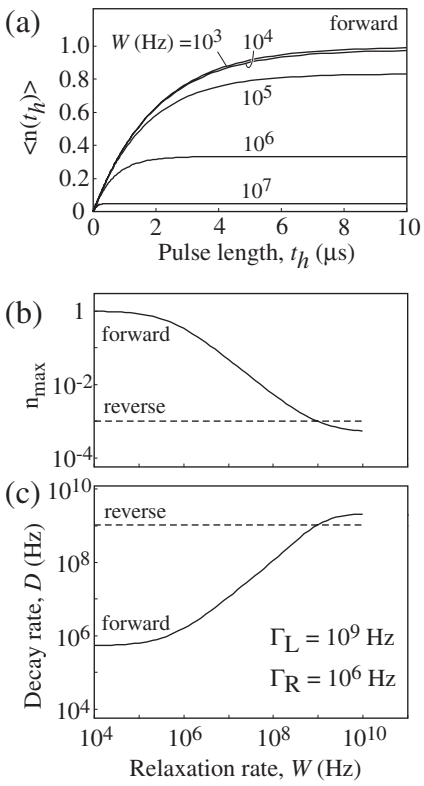

Fig. 2. (a) The average number of tunneling electrons $\langle n(t_h) \rangle$, calculated for the single-step pulse scheme. Each curve is approximated by a single exponential curve, $\langle n(t_h) \rangle \simeq n_{max}[1 - \exp(-Dt_h)]$, whose parameters n_{max} and D are plotted in (b) and (c), respectively.

$$\frac{\mathrm{d}\langle n(t_\mathrm{h})\rangle}{\mathrm{d}t_\mathrm{h}}|_{t_\mathrm{h}=0} = \Gamma_{\mathrm{L,e}}\Gamma_{\mathrm{R,e}}/(\Gamma_{\mathrm{L,e}} + \Gamma_{\mathrm{R,e}}). \quad (6)$$

We numerically calculated eq. (5), and approximated it to a single exponential function $\langle n(t_\mathrm{h})\rangle \simeq n_{\max}[1 - \exp(-Dt_\mathrm{h})]$. Here, $n_{\max}$ is the maximum number of tunneling electrons that can be obtained with a sufficiently long t_h, and D is the decay rate that describes the transient transport. D was determined so as to satisfy $\langle n(1/D)\rangle = n_{\max}(1 - 1/\mathrm{e})$. The $n_{\max}$ and D are plotted by solid lines in Figs. 2(b) and 2(c), respectively.

A similar calculation [dashed lines in Figs. 2(b) and 2(c)] was carried out for the reverse bias condition, where an electron is injected through a thicker barrier with slower rate Γ_R and is extracted through a thinner barrier with faster rate Γ_L. In this case, an electron easily enters the GS, and immediately ceases the transient transport.

As clearly seen from the figures, D and $n_{\max}$ for reverse bias are independent of W, while those for forward bias depend on W. Therefore, one can determine the tunneling rates from the reverse bias condition. D for reverse bias, D_{rev}, gives the total tunneling rate $D_{\mathrm{rev}} \sim \Gamma_{\mathrm{tot,g}} = \Gamma_{\mathrm{L,g}} + \Gamma_{\mathrm{R,g}} \sim \Gamma_{\mathrm{L,g}}$. Small $n_{\mathrm{max,rev}}$ reflects the asymmetry of the tunneling rates $\sim \Gamma_\mathrm{R}/\Gamma_\mathrm{L}$. In contrast, D_{for} for forward bias can vary from Γ_R to Γ_L, and $n_{\mathrm{max,for}}$ can vary from $\sim$1 to $\Gamma_\mathrm{R}/\Gamma_\mathrm{L}$ depending on W. Therefore, the decay rate D of the forward bias gives the relaxation rate W, provided that

$$\Gamma_\mathrm{L} \gtrsim W \gtrsim \Gamma_\mathrm{R}. \quad (7)$$

This condition can also be confirmed if $n_{\mathrm{max,for}}$ for forward bias is smaller than $\sim$1 but larger than $n_{\mathrm{max,rev}}$, or if D_{for} is smaller than D_{rev} but larger than Γ_R.

Another measurement for the tunneling rates can be performed by changing t_l with a sufficiently long t_h. The bias polarity can be either forward or reverse. Under the condition $t_\mathrm{h} \gg \Gamma_\mathrm{R}^{-1}$ at $V_\mathrm{g} = V_\mathrm{h}$, the QD ends up with the N_0-electron GS after the pulse, i.e. $\rho_\mathrm{e}(t_\mathrm{h}) = 0$ and $\rho_\mathrm{g}(t_\mathrm{h}) = 1$. During the next low-voltage application, an electron in the GS leaves the QD at a rate given by $\Gamma_{\mathrm{tot,g}} = \Gamma_{\mathrm{L,g}} + \Gamma_{\mathrm{R,g}}$. Since this extraction is required to see the transient current, the average number of tunneling electrons is simply given by

$$\langle n(t_\mathrm{l})\rangle = n_{\max}[1 - \exp(-\Gamma_{\mathrm{tot,g}}t_\mathrm{l})], \quad (8)$$

and $\Gamma_{\mathrm{tot,g}}$ can be obtained from this t_l dependence. Combining this with the conventional dc tunneling current, which is given by

$$I_\mathrm{g} = e\Gamma_{\mathrm{L,g}}\Gamma_{\mathrm{R,g}}/(\Gamma_{\mathrm{L,g}} + \Gamma_{\mathrm{R,g}}) \quad (9)$$

for the saturated current only through the GS,[7,8] allows us to determine $\Gamma_{\mathrm{L,e}}$ and $\Gamma_{\mathrm{R,e}}$.

2.2 *Double-step pulse measurement*

A better method to determine longer relaxation time, i.e., $W < \Gamma_{\mathrm{R,e}}$, is to apply a double-step voltage pulse, in which V_g is changed to three voltages, V_l, V_h and V_m as shown in Fig. 3(a).[3,9] Pumping and probing sequences are more clearly separated in this scheme. First, when $V_\mathrm{g} = V_\mathrm{l}$ [Fig. 3(b)], an empty QD is prepared during a sufficiently long period, t_l. When V_g is suddenly increased to V_h [Fig. 3(c)] so that both ES and GS are located below the Fermi energies, an electron enters either the ES or the GS. Once an electron enters either state, it can neither leave the dot, nor can another electron enter it. The QD is effectively isolated from the electrodes. If an electron has entered the ES, the ES may relax to the GS during this time. Therefore, the average number of electrons in the ES after this period, t_h, is approximately given by

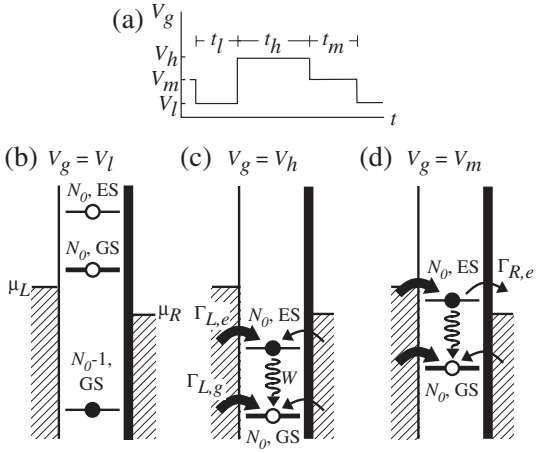

Fig. 3. (a) Schematic waveform of the double-step pulse. Energy diagram during the low (b), high (c), and middle (d) gate voltage.

$$\rho_{\mathrm{e,h}} = A\exp(-Wt_\mathrm{h})$$

for $t_\mathrm{h} \gg \Gamma_\mathrm{L}^{-1}$, where $A \simeq \frac{\Gamma_{\mathrm{L,e}}}{\Gamma_{\mathrm{L,e}}+\Gamma_{\mathrm{L,g}}}$. When V_g is changed to V_m [Fig. 3(d)], an electron in the ES can tunnel out to the drain, if the ES has not yet relaxed to the GS. This tunneling process can be described by eq. (1) with the initial conditions $\rho_\mathrm{e} = \rho_{\mathrm{e,h}}$ and $\rho_\mathrm{g} = 1 - \rho_{\mathrm{e,h}}$. With a sufficiently long duration, $t_\mathrm{m} \gg \Gamma_{\mathrm{R,e}}^{-1}$, for a complete readout, the average number of tunneling electrons, $\langle n\rangle$, can be written as

$$\langle n(t_\mathrm{h})\rangle = A'\exp(-Wt_\mathrm{h}), \quad (10)$$

where $A' = \Gamma_{\mathrm{R,e}}/\Gamma_{\mathrm{R,g}}$. Therefore the relaxation rate can be obtained from $\langle n(t_\mathrm{h})\rangle$. In this scheme, an electron is pumped into the ES at the rising edge of the pulse to V_h, and the electron in the ES is probed during the middle voltage V_m. The QD experiences the relaxation between the pumping and probing sequence.

Figure 4(a) shows a calculation of $\langle n(t_\mathrm{h})\rangle$ for the double-step pulse measurement with $\Gamma_{\mathrm{L,e}} = \Gamma_{\mathrm{L,g}} = 10^9\,\mathrm{Hz}$ and $\Gamma_{\mathrm{R,e}} = \Gamma_{\mathrm{R,g}} = 10^6\,\mathrm{Hz}$. We solved a series of rate equations that describe the transport for each period, and numerically obtained $\langle n(t_\mathrm{h})\rangle$. The $\langle n(t_\mathrm{h})\rangle$ can be approximated by a simple exponential curve $\langle n(t_\mathrm{h})\rangle = n_{\max}e^{-Dt_\mathrm{h}}$. The $n_{\max}$ and D are plotted in Figs. 4(b) and 4(c). Although the signal amplitude $n_{\max}$ is different for different bias polarities, the decay rate D is the same for both polarities. As clearly seen in Fig. 4(c), D directly gives the relaxation rate W for a wide condition $W \ll \Gamma_\mathrm{L}$.

3. Transient Current Measurement in a Quantum Dot

The two electrical pump and probe techniques were used to measure the relaxation time in QDs (artificial atoms). The QD we studied is located in a circular pillar (diameter of 0.5 μm) fabricated from an AlGaAs/InGaAs heterostructure.[10,11] Electrons are confined in an $In_{0.05}Ga_{0.95}As$

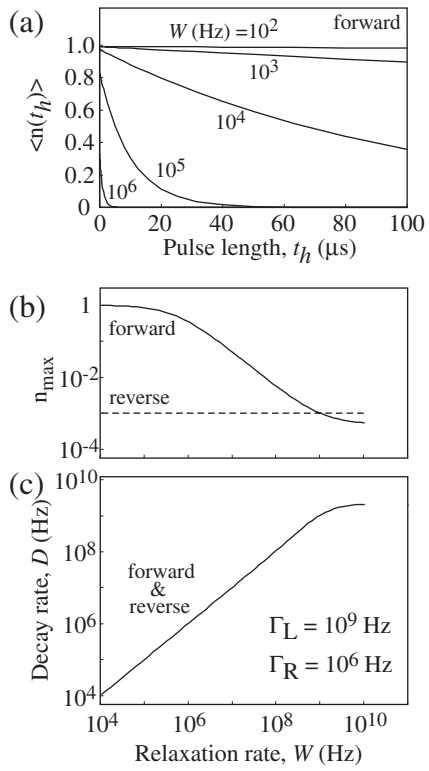

Fig. 4. (a) The average number of tunneling electrons $\langle n(t_h)\rangle$, calculated for double-step pulse scheme. Each curve is approximated by a single exponential curve, $\langle n(t_h)\rangle \simeq n_{max}\exp(-Dt_h)$, whose parameters n_{max} and D are plotted in (b) and (c), respectively.

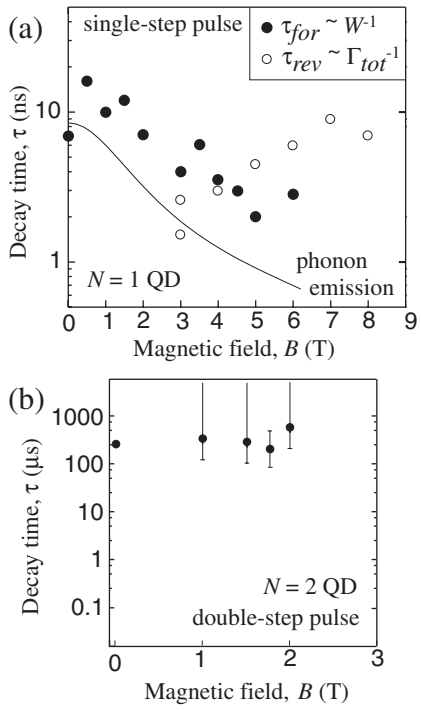

Fig. 5. (a) The decay time, D^{-1}, measured for $N = 1$ QD by the single-step pulse scheme. Solid and open circles are measured under the forward and reverse bias conditions, respectively. (b) The decay time, D^{-1}, measured for $N = 2$ QD by the double-step pulse scheme.

quantum well, and by approximately two-dimensional harmonic potentials in the lateral direction. A high-speed rectangular voltage-pulse (or double-step pulse) is introduced to a gate electrode through a low-loss coaxial cable. Due to a parasitic capacitance of the electrode (bonding pad) of the sample, the rise time of the pulse at the sample was $\tau_{rise} = 0.7$–2 ns, which was monitored by the reflected signal. The rectangular waveform contains a small ringing structure and fluctuations (less than 10% of the pulse height in the experiments), which slightly broaden the current peak and make energy selectivity worse.

Since a very small value of $\langle n\rangle$, which can be much smaller than one, is expected, we repeatedly apply pulses and measure the time-integrated current. The repetition frequency is typically 1–100 MHz for a single-step pulse, and 5 kHz–1 MHz for a double-step pulse. Practically, we always sweep the dc gate voltage V_h, (V_m) and V_l simultaneously by keeping the pulse height constant. A current peak appears when an ES is located in the transport window during the low-voltage interval of the pulse [see the corresponding energy diagrams in Figs. 1(d) and 3(d)]. The average number of tunneling electrons, $\langle n\rangle$, is obtained from the peak current divided by the repetition frequency and the elementary charge. When $\langle n\rangle$ is very small or when the repetition frequency is very low for the relaxation time measurement, many measurements of identical sweeps are averaged and smoothed to obtain a reliable peak current. For instance, the repetition frequency of 5 kHz and $\langle n\rangle \sim 0.5$ gives a current amplitude of only 0.4 fA. We need about one hour to average out the noise of our current meter ($\sim 20\,\mathrm{fA}/\sqrt{Hz}$). We clearly obtain transient current peaks for forward and reverse conditions under the application of single- and double-step pulses.

First, we applied single-step pulses to investigate the relaxation in the $N = 1$ QD system, which is the simplest case to study. The relaxation from the first ES to GS does not involve a spin-flip, and is accompanied by an acoustic phonon emission.[3] Figure 5(a) shows the decay time (the inverse of the decay rate, $\tau_{for} = D^{-1}$) of $\langle n(t_h)\rangle$ for forward bias (solid circles) and reverse bias (open circles) in the single-step pulse measurement. The magnetic field, B, was applied parallel to the current. Unfortunately, n_{max}, which varies from 5×10^{-3} to 5×10^{-2} and is always much smaller than 1, does not always change systematically, probably because the rise time of the pulse is comparable to Γ_L^{-1}, which fluctuates with B and the gate voltage in this sample. However, the decay time changes systematically with B as shown in Fig. 5(a), although it scatters by a factor of 2–3. As explained in the previous section, the decay rate for reverse bias gives the total tunneling rate. We see that $\tau_{rev} \sim \Gamma_{tot}^{-1}$ slightly increases with B. This dependence is qualitatively consistent with the B dependence of the conventional dc tunneling current given by eq. (9).

In contrast, the decay time for forward bias, τ_{for}, decreases with increasing B. We can roughly estimate $\Gamma_R^{-1} \sim 200$ ns from the conventional transport measurement, and τ_{for} is always much shorter than Γ_R^{-1}. For $B < 4$ T, where $\tau_{for} > \tau_{rev} \sim \Gamma_{tot}^{-1}$, we believe that the condition of eq. (7) is satisfied and τ_{for} approximately gives the relaxation time in this system. The observed dependence of τ_{for} almost follows the expected electron-phonon scattering time (solid line) in this QD,[3,12] indicating the validity of the relaxation

time experiment.

Next, we applied the double-step pulse measurement to investigate spin-flip energy relaxation in an $N = 2$ QD. In a low magnetic field $B < 2.5\,\mathrm{T}$, the $N = 2$ GS is a spin-singlet with two antiparallel-spin electrons occupying the 1s orbital, while the first ES is a spin-triplet with two parallel-spin electrons occupying the 1s and 2p orbitals. The relaxation from the triplet state to the singlet state requires a spin-flip. Figure 5(b) shows the decay time of $\langle n(t_\mathrm{h})\rangle$ measured with the double-step scheme, and gives the relaxation time in this QD. Although the error bar is quite large due to the current noise in our equipment, the spin-flip relaxation time is extremely long, $\sim 200\,\mu\mathrm{s}$, compared to the momentum relaxation time in $N = 1$ QD.

4. Conclusion

We described two electrical pump and probe techniques to investigate the relaxation time and tunneling rates separately. The measurable range in our setup is more than five orders of magnitude, and can be extended further by using tunable tunneling barriers and a low-noise current amplifier.

1) L. P. Kouwenhoven, C. M. Markus, P. L. McEuen, S. Tarucha, R. M. Westervelt and N. S. Wingreen: *Mesoscopic Electron Transport*, eds. L. L. Sohn, L. P. Kouwenhoven and G. Schön (Kluwer, Dordrecht, 1997) NATO ASI series E 345, pp. 105–214.
2) J. Weis, R. J. Haug, K. V. Klitzing and K. Ploog: Phys. Rev. Lett. **71** (1993) 4019.
3) T. Fujisawa, D. G. Austing, Y. Tokura, Y. Hirayama and S. Tarucha: Nature **419** (2002) 278.
4) T. Fujisawa, D. G. Austing, Y. Tokura, Y. Hirayama and S. Tarucha: Phys. Rev. Lett. **88** (2002) 236802.
5) T. Fujisawa, T. H. Oosterkamp, W. G. van der Wiel, B. W. Broer, R. Aguado, S. Tarucha and L. P. Kouwenhoven: Science **282** (1998) 932.
6) T. Fujisawa, Y. Tokura and Y. Hirayama: Phys. Rev. B **63** (2001) 081304.
7) T. Fujisawa, Y. Tokura and Y. Hirayama: Physica B **298** (2001) 573.
8) H. van Houten, C. W. J. Beenakker and A. A. M. Staring: *Single Charge Tunneling, Coulomb Blockade Phenomena in Nanostuctures*, eds. H. Grabert and M. H. Devoret (Plenum Press, New York, 1991) NATO ASI series B 294, pp. 167–216.
9) T. Fujisawa, Y. Tokura, D. G. Austing, Y. Hirayama and S. Tarucha: Physica B **314** (2002) 224.
10) S. Tarucha, D. G. Austing, T. Honda, R. J. van der Hage and L. P. Kouwenhoven: Phys. Rev. Lett. **77** (1996) 3613.
11) L. P. Kouwenhoven, T. H. Oosterkamp, M. W. S. Danoesastro, M. Eto, D. G. Austing, T. Honda and S. Tarucha: Science **278** (1997) 1788.
12) U. Bockelmann: Phys. Rev. B **50** (1994) 17271.